Published in final edited form as:
ACS Chem Biol. 2013 September 20; 8(9): 1907–1911. doi:10.1021/cb400340k.

Reduction of Human Defensin 5 Affords a High-Affinity Zinc-Chelating Peptide

Yunfei Zhang, **Fabien B. L. Cougnon**, **Yoshitha A. Wanniarachchi**, **Joshua A. Hayden**, and **Elizabeth M. Nolan***
Department of Chemistry, Massachusetts Institute of Technology, Cambridge, MA

Abstract

Human defensin 5 (HD5) is a 32-residue cysteine-rich host-defense peptide that exhibits three disulfide bonds in the oxidized form ($HD5_{ox}$). It is abundant in small intestinal Paneth cells, which release HD5 into the intestinal lumen and house a labile Zn(II) store of unknown function. Here we consider the redox properties of HD5 and report that the reduced form, $HD5_{red}$, is a metal-ion chelator. HD5 has a midpoint potential of −257 mV at pH 7.0. $HD5_{red}$ utilizes its cysteine residues to coordinate one equivalent of Zn(II) with an apparent K_{d1} value in the mid-picomolar range. Zn(II) or Cd(II) binding perturbs the oxidative folding pathway of $HD5_{red}$ to $HD5_{ox}$. Whereas $HD5_{red}$ is highly susceptible to proteolytic degradation, the Zn(II)-bound form displays resistance to hydrolytic breakdown by trypsin and other proteases. The ability of a reduced defensin peptide to coordinate Zn(II) provides a putative mechanism for how these peptides persist in vivo.

Defensins are ribosomally-synthesized, cysteine-rich, host-defense peptides that are biosynthesized by eukaryotes.(1) These peptides are celebrated for antimicrobial activity and other physiological roles that include immunomodulation and chemotatic function.(2) In the oxidized forms, human defensins exhibit regiospecific disulfide linkages that confer a triple-stranded β-sheet fold. Until recently, putative physiological roles for the reduced forms of these peptides have been largely overlooked. In vitro antibacterial activity assays with reduced murine cryptdin-4 revealed species-dependent antibacterial activity equal to or greater than that of the oxidized form.(3) Subsequent investigations demonstrated that reduced human β-defensin 1 (HBD-1) is colocalized with thioredoxin in the human colon,(4) and that living intestinal cells are able to reduce extracellular HBD-1 in a thioredoxin-dependent manner.(5) From the perspective of biological coordination chemistry, one striking feature of defensin peptides are the cysteine distributions, which are reminiscent of those observed in zinc-binding peptides such as metallothionein and the transcription factor GAL4.(6,7) We therefore questioned whether reduced defensins chelate zinc and, if so, whether this property is relevant in vivo.

To address the former notion, we focused on human defensin 5 (HD5, Figure 1), which is a 32-aa peptide produced by small intestinal Paneth cells,(8,9) and in the kidney, urinary, and female reproductive tracts.(10,11) We selected a Paneth cell defensin to evaluate in this exploratory work because these cells house a labile zinc store of unknown function.(12,13) Herein we report that (i) HD5 has a midpoint potential in the biological window, (ii) the reduced form of human defensin 5 ($HD5_{red}$) is a mid-picomolar-affinity zinc chelator, and

Corresponding Author: To whom the correspondence should be addressed. lnolan@mit.edu.

Supporting Information. Complete experimental methods, DynaFit scripts for dissociation constant determination, Tables S1–S5, and Figures S1–S11. Figure S10 exhibits HPLC traces of the peptides and Figure S11 provides the chemical structures of the Zn(II) indicators employed in this work. This material is available free of charge via the Internet at http://pubs.acs.org.

(iii) Zn(II) coordination affords protection of $HD5_{red}$ against proteolytic degradation by the intestinal protease trypsin and other proteases.

The oxidized form of HD5, hereafter $HD5_{ox}$, exhibits six cysteine residues that afford the disulfide linkages Cys_3—Cys_{31}, Cys_5—Cys_{20}, and Cys_{10}—Cys_{30}.(15) Whether $HD5_{red}$, the fully reduced species with six thiol residues, exists in vivo is currently unclear. To evaluate this possibility, we determined the midpoint potential of HD5 by incubating anaerobic solutions of $HD5_{red}$ or $HD5_{ox}$ in redox buffers with fixed $[DTT_{red}]$:$[DTT_{ox}]$ ratios that spanned the −230 to −290 mV range (75 mM HEPES, pH 7.0). Analytical HPLC of the equilibrium mixtures revealed varying ratios of peaks corresponding to $HD5_{red}$ and $HD5_{ox}$ that were dependent on the redox buffer composition (Supplementary Figure 1). Nernstian behavior was observed, and a midpoint potential of −257 mV was determined from analysis of the HPLC peak areas (Figure 2a). This value is well within the range expected for disulfide-containing peptides and proteins (Supplementary Table 1 and references therein), and falls within the redox potential range of the human gut (−150 to −300 mV).(16) Moreover, like HBD-1,(4) $HD5_{ox}$ is a substrate for mammalian Trx/TrxR. Incubation of $HD5_{ox}$ with human thioredoxin (Trx), rat liver thioredoxin reductase (TrxR), and NADPH resulted in formation of $HD5_{red}$ (Figure 2b, Supplementary Figure 2). These in vitro assays confirm that the midpoint potential of HD5 falls within the biological window, and support the notion that both the oxidized and reduced species of HD5 may exist under physiological conditions.

Under aerobic conditions, and in the absence of a reducing agent, $HD5_{red}$ is susceptible to oxidation. $HD5_{red}$ folds nearly quantitatively into $HD5_{ox}$ and a minor side-product (retention time ~ 13.0 min, not shown) over the course of an overnight incubation at room temperature at neutral pH (20 mM HEPES, pH 7.4). In contrast, incubation of $HD5_{red}$ with one equivalent of M(II) (M = Zn or its Group 12 congener Cd) under the same conditions results in the formation of new species (Figure 3a). LC-MS analysis of the acid-quenched incubations revealed the formation of ca. four prominent new peaks assigned as partially-oxidized regioisomers of HD5 containing one disulfide bridge and four thiols (calcd, 3584.66; found, 3584.65 – 3584.79; Supplementary Figure 2), along with peaks corresponding to $HD5_{red}$ and $HD5_{ox}$. As expected, addition of the reducing agent *tris*(2-carboxyethyl)phosphine to this mixture resulted in disappearance of all the new peaks corresponding to oxidized products (data not shown). These observations indicate that (i) $HD5_{red}$ coordinates both Zn(II) and Cd(II) in a similar manner, (ii) Zn(II)/Cd(II) binding is dynamic and fluctional, and (iii) metal binding perturbs oxidative folding of $HD5_{red}$ to $HD5_{ox}$. Moreover, the fact that each of the four prominent partially-oxidized peak contains a single disulfide bond suggests that each HD5 monomer employs four Cys residues to coordinate Zn(II) under these conditions. Whether the Zn(II):HD5 species are monomeric or oligomeric requires further investigation.

Titration of $HD5_{red}$ with M(II) at neutral pH monitored by optical absorption spectroscopy revealed formation of ligand-to-metal charge transfer bands (LMCT) centered at ca. 232 (Zn(II), $\varepsilon \sim 6{,}900\ M^{-1}cm^{-1}$ for 1:1 ratio) and 242 (Cd(II), $\varepsilon \sim 6{,}200\ M^{-1}cm^{-1}$ for 1:1 ratio) nm (Figure 3b,c), which confirmed the formation of Zn—S and Cd—S linkages, respectively. Moreover, MALDI-TOF mass spectrometry of Cd(II)/$HD5_{red}$ mixtures revealed *m/z* ratios consistent with the formation of 1:1 and 2:1 M(II):$HD5_{red}$ complexes (Supplementary Table 3).

With support for Zn(II) coordination in hand, we evaluated the affinity of $HD5_{red}$ for Zn(II) by conducting a series of anaerobic titrations where we competed the peptide and a colorimetric or fluorescent Zn(II) sensor of known Zn(II) affinity for the metal ion (75 mM HEPES, pH 7.4). Zincon, FluoZin-1 (FZ1), MagFura-2 (MF2) and Zinpyr-4 (ZP4) were

employed, and these Zn(II) sensors have K_d values that span the micromolar (Zincon, FZ1) to mid-picomolar (ZP4) range (Supporting Information). Titration of a 1:1 mixture of $HD5_{red}$ and Zincon or FZ1 resulted in no optical change of either Zn(II) indicator up to a 1:1 Zn(II)/$HD5_{red}$ ratio, demonstrating that $HD5_{red}$ coordinates one Zn(II) ion with higher (i.e. sub-micromolar) affinity than either Zincon or FZ1 (Supplementary Figure 3). In contrast, competition between $HD5_{red}$ and both MF2 and ZP4 was observed at 1:2 and 1:10 indicator/$HD5_{red}$ ratios, respectively (Figure 3d, Supplementary Figure 4). The titrations were fit to both 1:1 and 2:1 Zn(II):$HD5_{red}$ binding models using DynaFit (Supplementary Figure 4). Both models afforded apparent K_{d1} values in the mid-picomolar range, and the 2:1 model provided superior fits (K_{d1} = 509 ± 54 pM, MF-2; K_{d1} = 247 ± 23 pM, ZP4; from 2:1 model). The mid-picomolar apparent K_{d1} value was maintained with addition of 100 mM NaCl to the buffer (Supplementary Figure 4). The apparent K_{d2} values obtained from the data fitting spanned the mid-nanomolar range (Supplementary Figure 4). These values are lower than the apparent K_{d2} values predicted from the Zincon/FZ-1 experiments and may reflect the inability of the indicators to report on two K_d values that differ by several orders of magnitude. In total, the results from the MF2/ZP4 competition titrations indicate that $HD5_{red}$ coordinates one zinc ion with mid-picomolar affinity, and suggest a second zinc-binding event with substantially weaker affinity.

Because Zn(II) is a spectroscopically-silent $3d^{10}$ metal ion, the nature of M(II) binding was further investigated by using cobalt(II), a $3d^7$ metal ion, as a spectroscopic probe.(17) Well-established correlations between Co(II) ligand field transitions and coordination geometries exist, and Co(II) has been routinely employed to probe the coordination modes of zinc-binding peptides including zinc fingers(18) and metallothioneins.(19) Anaerobic titration of $HD5_{red}$ with Co(II) resulted in a blue solution at sub-stoichiometric equivalents of the metal ion and a green solution following addition of higher equivalents of Co(II) (Supplementary Figure 5). These solutions turned yellow following exposure to the atmosphere, an observation consistent with oxidation of the Co(II) center. At <1 equiv of Co(II), a LMCT band at 305 nm (ε ~ 5,900 $M^{-1}cm^{-1}$), with a shoulder at 400 nm (ε ~ 4,990 $M^{-1}cm^{-1}$), formed in addition to three well-resolved *d—d* transitions at 612 (ε ~ 580 $M^{-1}cm^{-1}$), 678 (ε = 720 $M^{-1}cm^{-1}$), and 736 (ε ~ 660 $M^{-1}cm^{-1}$) (Figure S6). At >1 equivalent of Co(II), the intensities of the LMCT band and *d—d* transitions increased, and a slight red-shift in the *d—d* transition at 678 nm occurred. These electronic transitions are similar to those reported for Co(II)-tetrathiolate species including metallothionein and well-defined small-molecule Co(II) complexes (Supplementary Table 5 and references therein). These results support the notion that the $HD5_{red}$ scaffold affords Co(II) tetrathiolate species, and suggest a distorted T_d geometry for Co(II) bound to HD5. Further spectroscopic studies and magnetic characterization are necessary to ascertain whether Co(II)-thiolate clusters, as observed for metallothionein and GAL4, form.

Lastly, we questioned how Zn(II) coordination influences proteolytic stability of the HD5 peptide backbone. Trypsin is responsible for proteolytic processing of the HD5 propeptide in vivo and release of mature $HD5_{ox}$.(20) $HD5_{ox}$ is therefore resistant to degradation by this enzyme(21,22) as a result of its triple-stranded β-sheet fold whereas linearized $HD5_{red}$ is susceptible to proteolytic breakdown (Figure 4). To evaluate whether Zn(II) coordination influences the trypsin susceptibility of $HD5_{red}$, we pre-incubated $HD5_{red}$ with varying equivalents of Zn(II) prior to conducting the trypsin degradation assay, and observed attenuation of proteolysis when >1 equiv of Zn(II) was added (Figure 4). Control assays employing HD5-TE, which has all six Cys residues capped by iodoacetamide and cannot form Zn—S bonds, confirmed that Zn(II) addition to the assay mixture did not compromise trypsin activity (Supplementary Figure 7). Furthermore, degradation assays employing chymotrypsin and proteinase K revealed that Zn(II) also provides protection of the HD5 backbone from these proteases (Supplementary Figures 8,9).

In summary, HD5 has a midpoint potential within the biological window, and the oxidized form is a substrate for mammalian Trx/TrxR. $HD5_{red}$ provides mid-picomolar-affinity Zn(II) chelation, and the Zn(II) complex exhibits resistance to protease-catalyzed hydrolytic breakdown. Metal-dependent reduction of protease-catalyzed degradation provides a plausible mechanism by which reduced defensins persist and exert functional activity in vivo. Along such lines, how protease-susceptible reduced HBD-1 exists in vivo has been questioned.(23) To the best of our knowledge, this investigation constitutes the first assessment of defensin midpoint potential and zinc chelating ability, and points to a putative and unappreciated new role for defensin family members in mammalian physiology. Thus, it will be valuable to further probe the structural and functional properties of Zn(II):$HD5_{red}$ and extend such analyses to other defensin family members. Moreover, it will be important to elucidate whether defensins participate in the biology of Zn(II) or other transition metal ions via chelation-dependent or -independent mechanisms. Along these lines, upregulation of plant defensin at the transcriptional level has been observed following Zn(II) exposure.(24) Of relevance to this work are the defensin and zinc stores harbored by intestinal Paneth cells. Nutritional Zn(II) deficiency in humans has been correlated with a reduction in both Paneth cell granules and HD5 immunoreactivity.(25) Thus, it will be intriguing to decipher whether Paneth cell host-defense peptides and Zn(II) have synergistic function.

METHODS

General Materials and Methods

The materials and methods employed in this work are detailed in the Supporting Information.

Midpoint Potential Determination

The midpoint potential (E_m) of HD5 was determined by incubating either $HD5_{red}$ or $HD5_{ox}$ in buffers poised at defined redox potentials prepared using the reduced (DTT_{red}) and oxidized (DTT_{ox}) forms of dithiothreitol (DTT) (75 mM HEPES, pH 7.0; anaerobic glovebox) as described in the Supporting Information. Buffers with redox potentials spanning the −230 to −290 mV range were prepared in 5-mV increments. A 100-μL solution of 25 μM $HD5_{red}$ (or $HD5_{ox}$) was prepared in each redox buffer and the samples were incubated in the glovebox at room temperature (ca. 22 °C) for 20 h in order for equilibrium to be reached. At t = 20 h, the samples were quenched with 10 μL of 6% aqueous TFA, removed from the glovebox, centrifuged (13,000 rpm × 10 min, 4 °C), and the resulting supernatants were analyzed by HPLC. The percentages of $HD5_{red}$ and $HD5_{ox}$ at equilibrium were determined by integrating the HPLC peak areas ($HD5_{red}$, 19.9 min retention time; $HD5_{ox}$, 14.4 min retention time).

Thioredoxin Activity Assays

Four 100-μL solutions containing 20 μM $HD5_{ox}$, 15 μM human thioredoxin (Trx), 0.5 μM rat liver thioredoxin reductase (TrxR), 1 mM NADPH, and 2 mM EDTA (100 mM potassium phosphate buffer, pH 7.0) were prepared and the conversion of $HD5_{ox}$ to $HD5_{red}$ monitored at different time points. The activity assay was initiated by adding Trx to the reaction last. The mixtures were incubated at room temperature, and each reaction was quenched at a different time point (t = 0, 10, 20, 30 sec) by addition of 10 μL of 6% aqueous TFA. The acidified solutions were immediately vortexed and centrifuged (13,000 rpm × 10 min, 4 °C), and the resulting supernatants were immediately analyzed by HPLC.

HPLC Assays for Zinc and Cadmium Coordination

Solutions (100 μL) containing 50 μM $HD5_{red}$ and either 1.0 equiv of Zn(II) or 1.0 equiv of Cd(II), or no added metal, were prepared at pH 7.4 (75 mM HEPES, 100 mM NaCl, not Ar-purged) under aerobic conditions. The resulting solutions were incubated overnight on the bench top (capped 1.7-mL microcentrifuge tubes) at room temperature and subsequently acidified with 10 μL of 6% aqueous TFA. The acidified solutions were vortexed, centrifuged (13,000 rpm × 10 min, 4 °C), and the supernatants analyzed by HPLC.

Optical Absorption Spectroscopy

In a typical optical absorption titration of $HD5_{red}$ with Zn(II) or Cd(II), a 200-μL solution of 20 μM $HD5_{red}$ (20 mM HEPES, 100 μM TCEP, pH 7.4, Ar-purged) was prepared in a quartz cuvette. Aliquots of a concentrated Zn(II) or Cd(II) stock solution were added. The cuvette was capped and mixed gently after each M(II) addition, and the optical absorption spectrum recorded. The total change in volume during each titration was less than 2%. A rising baseline and decrease in absorption intensity at ca. A_{230}, suggesting precipitate formation, was routinely observed after addition of ≥2 equiv of Zn(II) to ≥20 μM $HD5_{red}$ under these conditions.

For a typical Co(II)-binding titration, a 200-μL solution of 50 – 150 μM $HD5_{red}$ (75 mM HEPES, pH 7.4) was prepared in an anaerobic quartz cuvette in the glovebox and the optical absorption spectrum recorded. Aliquots from a concentrated Co(II) stock solution were added in the glovebox. After each Co(II) addition, the cuvette was sealed and inverted gently for mixing before recording the optical absorption spectrum. The total change in volume during the titration was less than 2%. No precipitation was observed with Co(II) addition under these experimental conditions.

Zinc Competition Experiments with $HD5_{red}$ and Zn(II) Sensors

All Zn(II) competition experiments were performed under anaerobic conditions in the glovebox under a nitrogen atmosphere as described in the Supporting Information.

Protease Susceptibility Assays

To determine whether Zn(II) modulates the susceptibility of $HD5_{red}$ to proteolytic degradation, a solution containing 50 μM $HD5_{red}$ in the presence of 1.2 equiv of Zn(II) was prepared and incubated at room temperature (100 mM Tris-HCl, 20 mM $CaCl_2$, 0.001% Triton-X 100, 5 mM TCEP, pH 8.2). The protease of interest was added to initiate the reaction (final concentration: trypsin, 0.25 μg/mL; chymotrypsin, 0.25 μg/mL; proteinase K, 1 μg/mL). Aliquots (50 μL) were removed at t = 1, 2, 5, 15, 30, and 60 min and immediately quenched with 5 μL of 6% TFA, vortexed, and stored at −20 °C prior to HPLC analysis. In parallel, assays in which Zn(II) was omitted from the reaction were also performed. In addition, control assays using HD5-TE, which cannot bind Zn(II), instead of $HD5_{red}$ were conducted for each protease to confirm that Zn(II) addition did not perturb protease activity.

Supplementary Material

Refer to Web version on PubMed Central for supplementary material.

Acknowledgments

This work was supported by NIH Grant DP2OD007045 from the Office of the Director, the Searle Scholars Program (Kinship Foundation), and the Department of Chemistry at MIT. We thank S. An, M. Brophy, A. Wan, and A. Wommack for technical assistance.

REFERENCES

1. Lehrer RI, Lu W. α-Defensins in human innate immunity. Immunol. Rev. 2012; 245:84–112. and references therein. [PubMed: 22168415]
2. Ganz T. Defensins: Antimicrobial peptides of innate immunity. Nat. Rev. Immunol. 2003; 3:710–720. [PubMed: 12949495]
3. Masuda K, Sakai N, Nakamura K, Yoshioka S, Ayabe T. Bactericidal activity of mouse α-defensin cryptdin-4 predominantly affects noncommensal bacteria. J. Innate Immun. 2011; 3:315–326. [PubMed: 21099205]
4. Schroeder BO, Wu Z, Nuding S, Groscurth S, Marcinowski M, Beisner J, Buchner J, Schaller M, Stange EF, Wehkamp J. Reduction of disulphide bonds unmasks potent antimicrobial activity of human β-defensin 1. Nature. 2011; 469:419–423. [PubMed: 21248850]
5. Jaeger SU, Schroeder BO, Meyer-Hoffert U, Courth L, Fehr SN, Gersemann M, Stange EF, Wehkamp J. Cell-mediated reduction of human β-defensin 1: a major role for mucosal thioredoxin. Musocal Immunol. 2013 ahead of print.
6. Vallee BL, Auld DS. Zinc coordination, function, and structure of zinc enzymes and other proteins. Biochemistry. 1990; 29:5647–5659. [PubMed: 2200508]
7. Maret W, Li Y. Coordination dynamics of zinc in proteins. Chem. Rev. 2009; 109:4682–4707. [PubMed: 19728700]
8. Porter EM, Liu L, Oren A, Anton PA, Ganz T. Localization of human intestinal defensin 5 in Paneth cell granules. Infect. Immun. 1997; 65:2389–2395. [PubMed: 9169779]
9. Clevers HC, Bevins CL. Paneth cells: maestros of the small intestinal crypts. Annu. Rev. Physiol. 2013; 75:289–311. 311 and references therein. [PubMed: 23398152]
10. Spencer JD, Hains DS, Porter E, Bevins CL, DiRosario J, Becknell B, Wang H, Schwaderer AL. Human alpha defensin 5 expression in the human kidney and urinary tract. PlosONE. 2012; 7:e31712.
11. Quayle AJ, Porter EM, Nussbaum AA, Wang YM, Brabec C, Yip K-P, Mok SC. Gene expression, immunolocalization, and secretion of human defensin-5 in human female reproductive tract. Am. J. Pathol. 1998; 152:1247–1258. [PubMed: 9588893]
12. Dinsdale D. Ultrastructural localization of zinc and calcium within the granules of rat Paneth cells. J. Histochem. Cytochem. 1984; 32:139–145. [PubMed: 6693753]
13. Giblin LJ, Chang CJ, Bentley AF, Frederickson C, Lippard SJ, Frederickson CJ. Zinc-secreting Paneth cells studies by ZP fluorescence. J. Histochem. Cytochem. 2006; 54:311–316. [PubMed: 16260591]
14. Wommack AJ, Robson SA, Wanniarachchi YA, Wan A, Turner CJ, Wagner G, Nolan EM. NMR solution structure and condition-dependent oligomerization of the antimicrobial peptide human defensin 5. Biochemistry. 2012; 51:9624–9637. [PubMed: 23163963]
15. Szyk A, Wu Z, Tucker K, Yang D, Lu W, Lubkowski J. Crystal structures of human alpha-defensins HNP4, HD5, and HD6. Protein Sci. 2006; 15:2749–2760. [PubMed: 17088326]
16. Wilson, M. Microbial Inhabitants of Humans. Vol. Chapter 7. Cambridge U.K.: Cambridge University Press; 2005. The gastrointestinal tract and its indigenous microbiota; p. 251-317.
17. Maret W, Vallee BL. Cobat as a probe and label of proteins. Methods Enz. 1993; 226:52–71.
18. Krizek BA, Merkle DL, Berg JM. Ligand variation and metal ion binding specificity in zinc finger peptides. Inorg. Chem. 1993; 32:937–940.
19. Vašák M, Kägi JHR. Metal thiolate clusters in cobalt(II)-metallothionein. Proc. Natl. Acad. Sci. U. S. A. 1981; 78:6709–6713. [PubMed: 6273885]
20. Ghosh D, Porter E, Shen B, Lee SK, Wilk D, Drazba J, Yadav SP, Crabb JW, Ganz T, Bevins CL. Paneth cell trypsin is the processing enzyme for human defensin 5. Nature Immunol. 2002; 3:583–590. [PubMed: 12021776]
21. Rajabi M, de Leeuw E, Pazgier M, Li J, Lubkowski J, Lu W. The conserved salt bridge in human α-defensin 5 is required for its precursor processing and proteolytic stability. 2008; 283:21509–21518.

22. Wanniarachchi YA, Kaczmarek P, Wan A, Nolan EM. Human defensin 5 disulfide array mutants: Disulfide bond deletion attenuates antibacterial activity against. Staphylococcus aureus. 2011; 50:8005–8017.

23. Schroeder BO, Stange EF, Wehkamp J. Waking the wimp: Redox-modulation activates human beta-defensin 1. Gut Microbes. 2011; 2:262–266. [PubMed: 21983064]

24. Mirouze M, Sels J, Richard O, Czernic P, Loubet S, Jacquier A, Francois IEJA, Cammue BPA, Lebrun M, Berthomieu P, Marquès L. A putative novel role for plant defensins: a defensin from the zinc hyper-accumulating plant, *Arabidopsis halleri* confers zinc tolerance. Plant J. 2006; 47:329–342. [PubMed: 16792695]

25. Kelly P, Feakins R, Domizio P, Murphy J, Bevins C, Wilson J, McPhail G, Poulsom R. Paneth cell granule depletion in the human small intestine under infective and nutritional stress. Clin. Exp. Immunol. 2004; 135:303–309. [PubMed: 14738460]

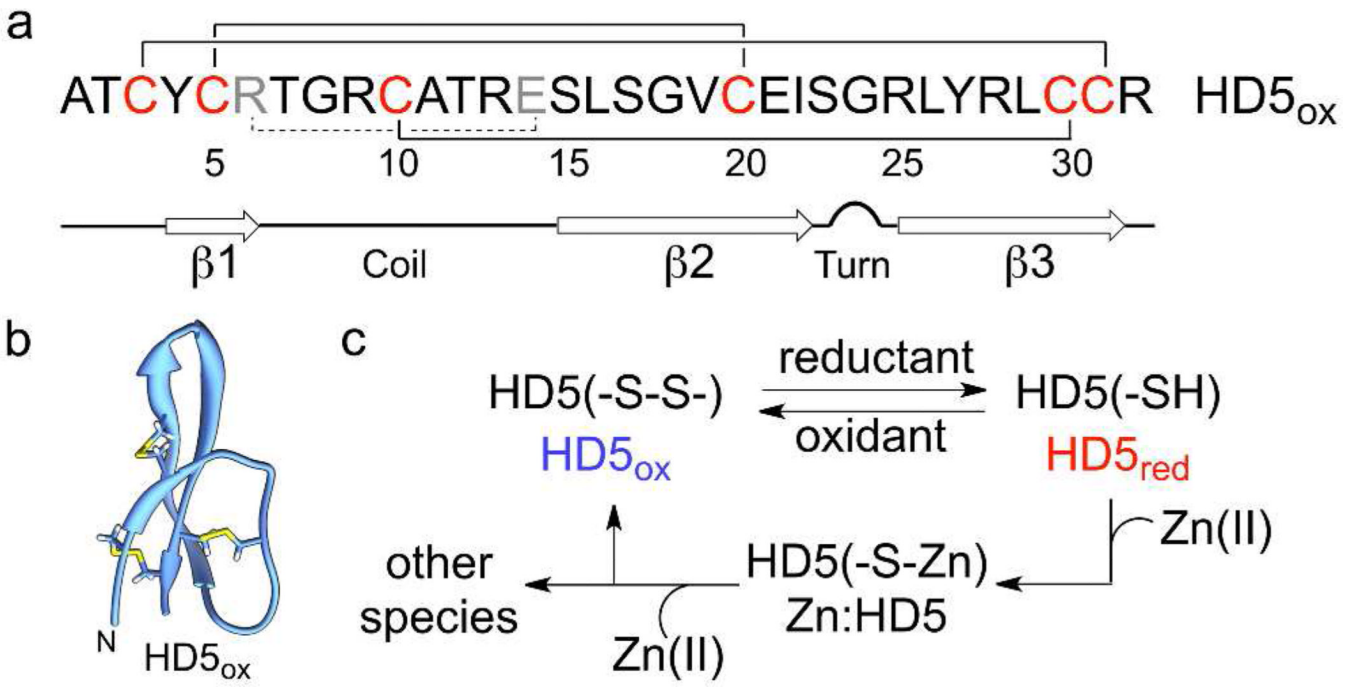

Figure 1.

HD5 is a cysteine-rich host-defense peptide. (a) Primary amino acid sequence of HD5. The numbers indicate the amino acid position. The Cys residues are red and the solid lines indicate the native disulfide bonds of $HD5_{ox}$. The residues of the Arg^{6}—Glu^{14} salt bridge (dashed line) are grey. (b) NMR solution structure of $HD5_{ox}$ (PDB: 2LXZ).(10) (c) Working model for this investigation. After reduction of the disulfide bonds, $HD5_{red}$ coordinates Zn(II) via its Cys residues. Zn(II) release results in the formation of $HD5_{ox}$ and other partially-oxidized species.

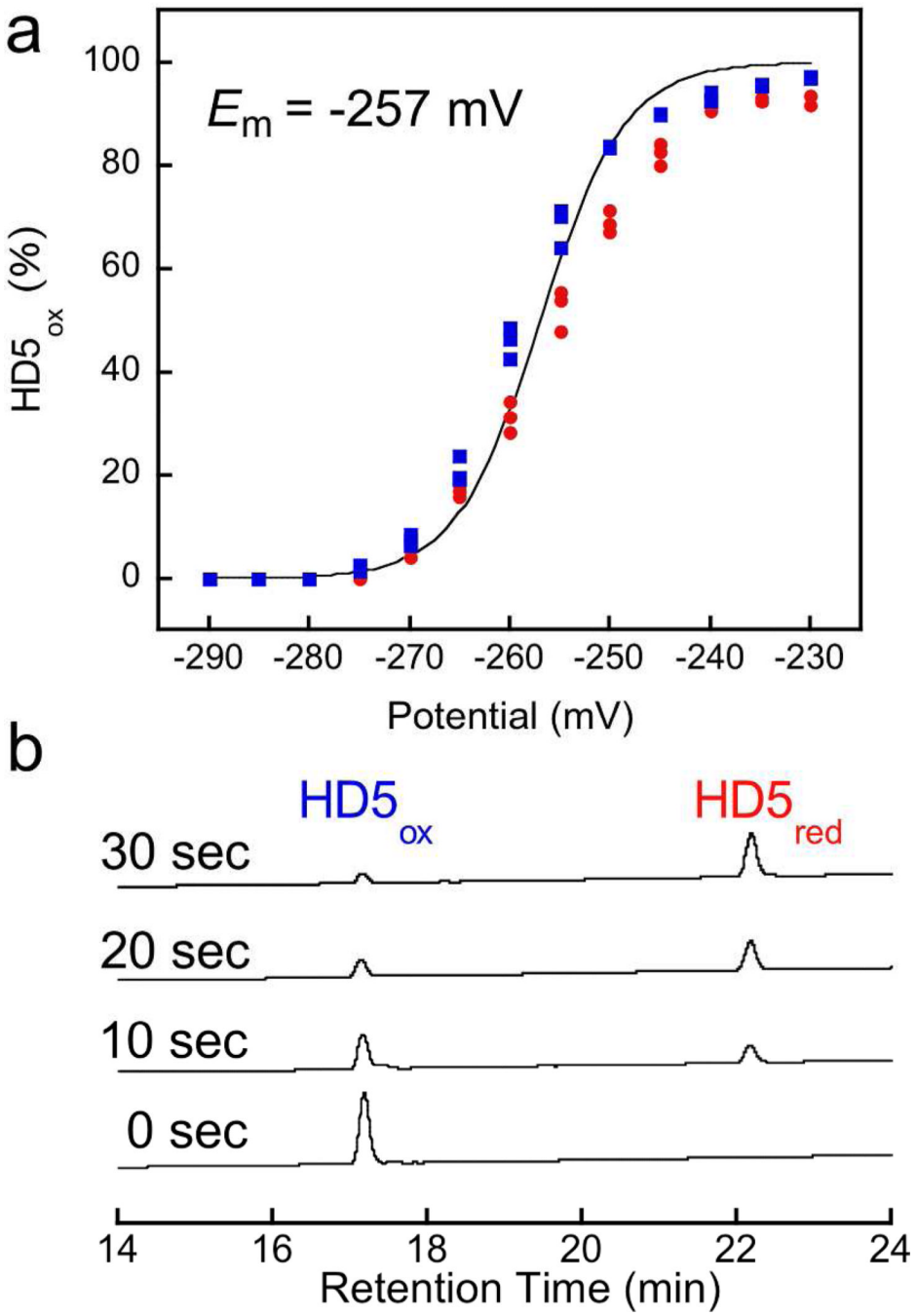

Figure 2.

Reduction of $HD5_{ox}$ occurs chemically and enzymatically. (a) Percentage of $HD5_{ox}$ at equilibrium after incubation of 25 μM $HD5_{ox}$ (blue squares) or 25 μM $HD5_{red}$ (red circles) in dithiothreitol-based redox buffers with defined redox potentials (75 mM HEPES, pH 7.0). The circles and squares are the experimental data and the line represents the global fit. (b) Analytical HPLC traces (220 nm) showing the time-dependent reduction of 20 μM $HD5_{ox}$ to $HD5_{red}$ in the presence of 15 μM human Trx, 0.5 μM rat liver TrxR and 1 mM NADPH (100 mM potassium phosphate, 2 mM EDTA, pH 7.0). Data from control assays are presented in Figure S2.

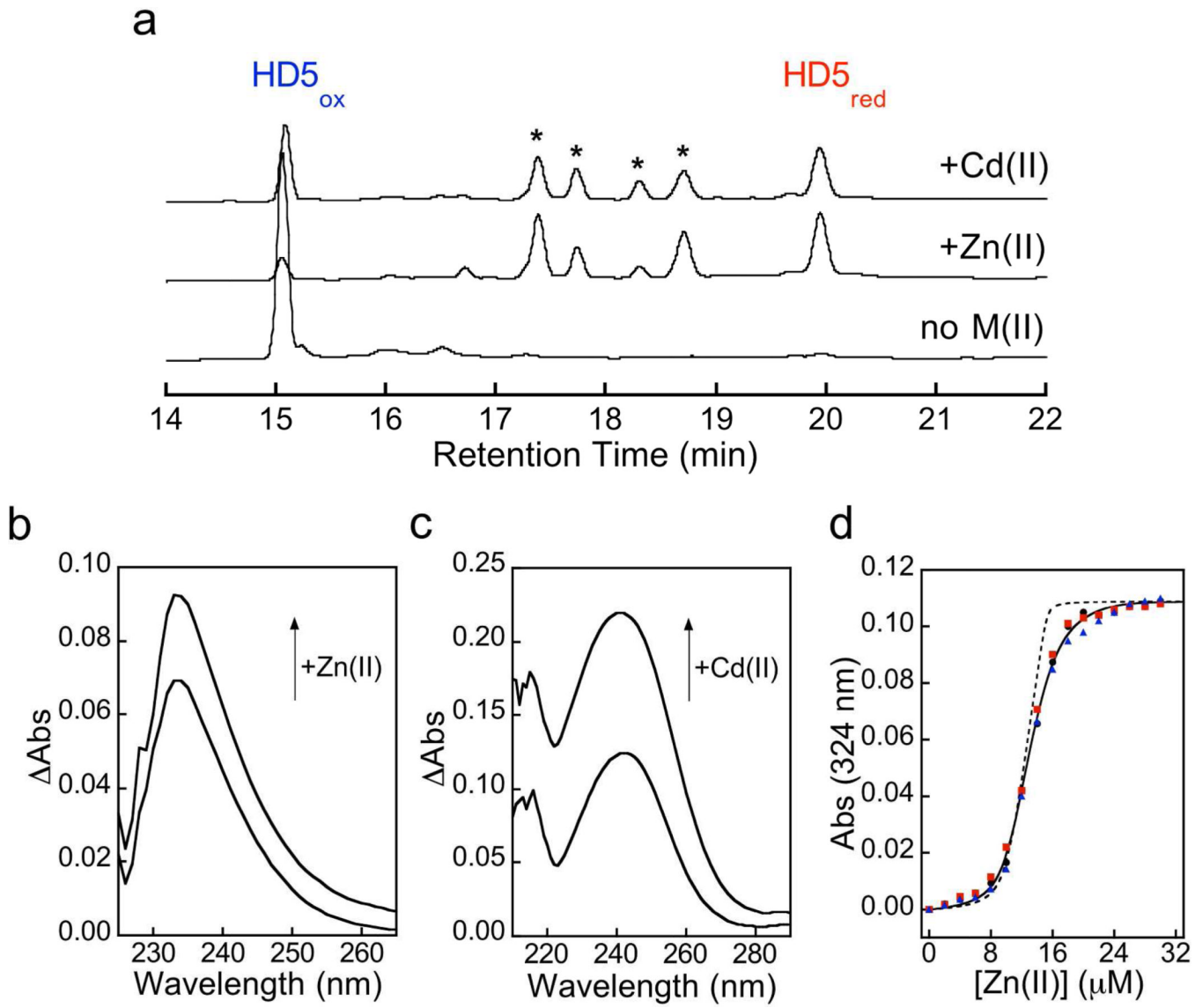

Figure 3.

$HD5_{red}$ chelates Zn(II) and Cd(II) via its cysteine residues. (a) Analytical HPLC traces (220 nm) of samples from an overnight incubation of 50 μM $HD5_{red}$ in the absence or presence of 1.0 equiv of Zn(II) or Cd(II) (75 mM HEPES pH 7.4, rt). The * indicate partially-oxidized species that were identified by mass spectrometry (Table S2). (b) Optical absorption difference spectra of 10 μM $HD5_{red}$ in the presence of 1.0 and 2.0 equiv of Zn(II) (20 mM HEPES, 100 μM TCEP, pH 7.4, rt). (c) Optical absorption difference spectra of 20 μM $HD5_{red}$ in the presence of 1.0 and 2.0 equiv of Cd(II) (20 mM HEPES, 100 μM TCEP, pH 7.4, rt). (d) Competition of 10 μM $HD5_{red}$ and 10 μM MF2 for Zn(II) (75 mM HEPES, pH 7.4, anaerobic, rt). The circles, squares, and triangles correspond to three independent titrations. The black line is the global fit to the three data sets obtained by using a two-site binding model (K_{d1} = 509 ± 54 pM; K_{d2} = 353 ± 25 nM). The dashed line represents the fit obtained by using a one-site binding model (K_{d1} = 331 ± 142 pM).

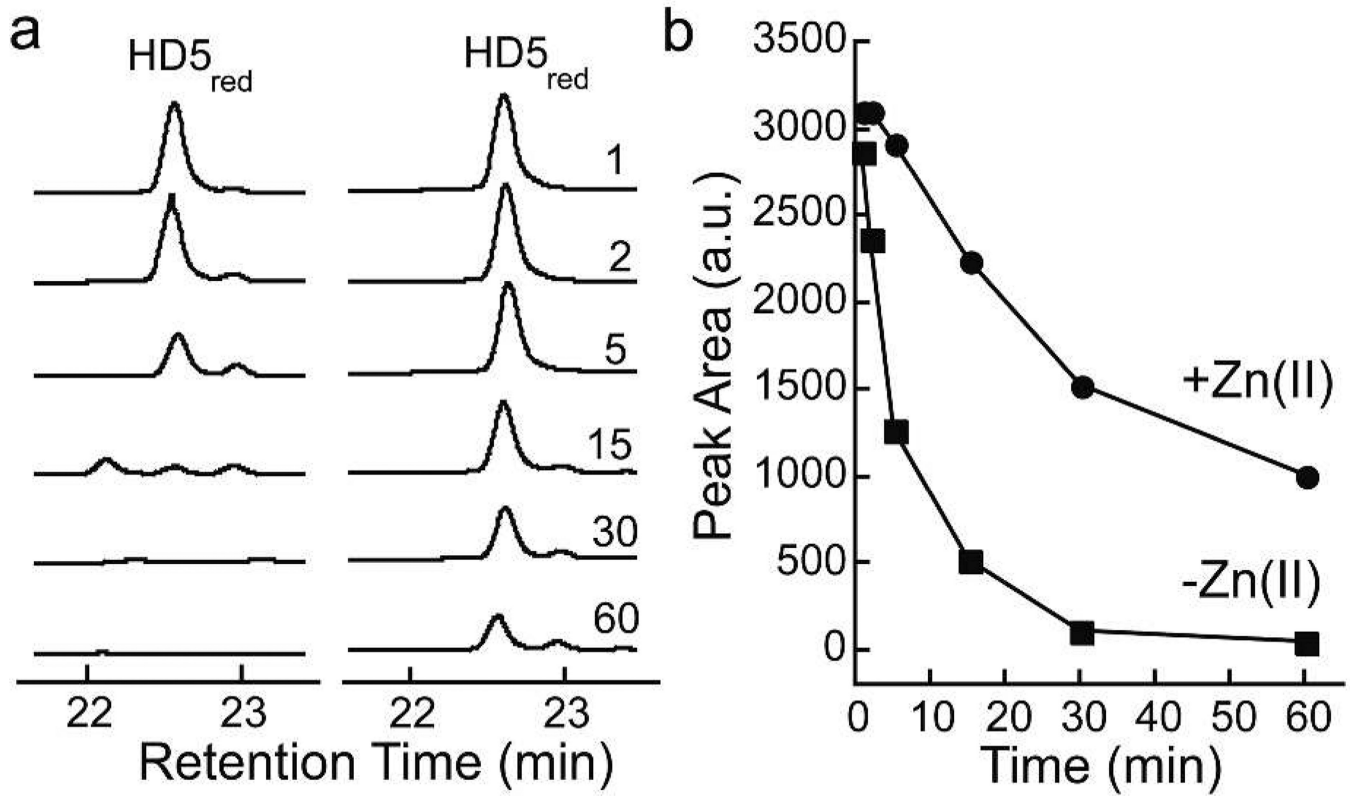

Figure 4.

Trypsin-catalyzed hydrolysis of 50 μM $HD5_{red}$ in the absence and presence of 1.2 equiv of Zn(II). (a) Analytical HPLC traces (220 nm). Left: no Zn(II) added; right: addition of Zn(II). The reactions were quenched at t = 1, 2, 5, 15, 30, and 60 min (units not shown). (b) Integrated $HD5_{red}$ peak area versus time. These data correspond to the peaks exhibited in Panel A. Full HPLC chromatograms and HD5-TE controls are presented in Figure S7.